Enhanced spin-orbit torques in Pt/Co/Ta heterostructures

Seonghoon Woo, Maxwell Mann, Aik Jun Tan, Lucas Caretta, and Geoffrey S. D. Beach

Citation: Applied Physics Letters **105**, 212404 (2014); doi: 10.1063/1.4902529
View online: http://dx.doi.org/10.1063/1.4902529
View Table of Contents: http://scitation.aip.org/content/aip/journal/apl/105/21?ver=pdfcov
Published by the AIP Publishing

Enhanced spin-orbit torques in Pt/Co/Ta heterostructures

Seonghoon Woo, Maxwell Mann, Aik Jun Tan, Lucas Caretta, and Geoffrey S. D. Beach[a)]
Department of Materials Science and Engineering, Massachusetts Institute of Technology, Cambridge, Massachusetts 02139, USA

(Received 20 October 2014; accepted 11 November 2014; published online 25 November 2014)

Spin-orbit torques (SOTs) are studied in perpendicularly magnetized ultrathin Co films sandwiched between two heavy metals, Pt and Ta. A significant enhancement of the Slonczewski-like torque is achieved by placing dissimilar metals with opposite spin Hall angles on opposite sides of the ferromagnet. SOTs were characterized through harmonic measurements and the contribution by the Ta overlayer was isolated by systematically varying its thickness. An effective spin Hall angle of up to 34% is observed, along with a sizable field-like torque that increases with increasing Ta layer thickness. Current-induced switching measurements reveal a corresponding increase in switching efficiency, suggesting that by engineering both interfaces in trilayer structures, the SOTs can be significantly improved. © *2014 AIP Publishing LLC*. [http://dx.doi.org/10.1063/1.4902529]

Current-induced torques in ultrathin ferromagnets sandwiched by a heavy metal and an oxide have been of significant recent interest for highly efficient magnetization switching[1–8] and domain wall motion.[9–14] In these systems, strong spin-orbit torques (SOTs) can arise through the spin Hall effect (SHE)[2–4,13,15–19] and the Rashba effect[11,20–23] at the heavy-metal/ferromagnet interface, which can be exploited for low-power operation of spintronic memory and logic devices. These effects produce both a Slonczewski-like torque[24–26] that drives magnetization switching, and a field-like torque[27] whose effective field lies parallel to the interface and orthogonal to the current flow direction. The Slonczewski-like torque is similar to the spin-transfer torque in conventional current-perpendicular-to-plane geometries, and is conveniently parameterized by an effective spin Hall angle θ_{SH}, which refers to the ratio of out-of-plane spin current to in-plane charge current. Since the efficiency of SOT switching relates directly to the magnitude of θ_{SH}, much effort is currently directed at identifying materials and interfaces for which θ_{SH} is large.

Pt and Ta have been the most widely examined spin Hall metals due to their relatively high spin Hall angles, $\sim+0.07$ for Pt (Refs. 2, 13, and 17) and ~-0.12 to -0.15 for β-Ta (Ref. 3) and their simultaneous utility as underlayers that promote perpendicular magnetic anisotropy (PMA) in thin Co and CoFe(B) films. Recent work has aimed to increase the SHE efficiency by seeking other heavy metals and alloys with larger θ_{SH}, with a record of $+0.3$ having been reported for beta phase W.[4] To date, most work has focused on heavy-metal/ferromagnet/oxide trilayer structures, where the oxide layer plays the role of breaking inversion symmetry, without actively contributing to the SOTs. One could therefore anticipate that by engineering SOTs at both interfaces, the efficiency of current-induced torques could be further increased using already-known spin Hall materials.

Here, we examine SOTs in ultrathin Co films sandwiched between two heavy metals, Pt and Ta, whose spin Hall angles are of opposite sign. In this case, the spin Hall effect at the top and bottom interfaces are expected to work in concert to enhance the total Slonczewski-like torque. We perform harmonic measurements of the current-induced effective fields[21,28–31] and characterize current-induced switching in a series of Pt/Co/Ta stacks with PMA. We find that the effective fields and switching efficiency increase significantly with increasing Ta overlayer thickness, yielding an effective spin Hall angle of up to 0.34, which is the largest value observed to date in a metallic system.

Figure 1 shows the stack structure and corresponding hysteresis loops measured using vibrating sample magnetometry. A series of Ta(4 nm)/Pt(3 nm)/Co(0.9 nm)/Ta(t) tri-layer structures capped by 1.5 nm of TaOx was prepared by dc-magnetron sputtering onto thermally oxidized Si. The nominal thickness t_{Ta} of the Ta metal top layer varied from 0.5 nm to 4 nm (Fig. 1(a)). Sputter deposition was performed at room temperature under 3 mTorr Ar at a background pressure of $\sim2\times10^{-7}$ Torr for the metal layers. The TaOx overlayer was then deposited by reactive sputtering in an oxygen partial pressure of $\sim5\times10^{-5}$ Torr. These films all exhibited PMA in the as-deposited state (Figs. 1(b) and 1(c)), with saturation magnetization M_S of 780, 750, 660, and 530 emu/cm^3 for $t_{Ta}=0.5$, 1, 2, and 4 nm, respectively. The measured M_s is roughly half the bulk value for Co, which we attribute to Ta intermixing at the Co/Ta interface as discussed below.

X-ray photoelectron spectroscopy (XPS) sputter-depth profiling was performed to extract the depth-dependent material compositions. Here, a thicker Pt layer was used (15 nm) to minimize the contribution of the bottom Ta adhesion layer to the XPS spectra. Figure 2 shows the normalized intensity of Co, O, Pt, and Ta signals extracted by integrating the relative areas of the Ta 4f, Co 2p, Pt 4f, and O 1s peaks in XPS spectra acquired periodically during sputter etching (see supplementary material for spectra and analysis details[32]). All four samples show significant overlap of Co and Ta signals indicating intermixing between Ta and Co, consistent with the reduced M_s. In Fig. 2(a), with $t_{Ta}=0.5$ nm, the normalized O signal is at ~20% of its maximum value when the Co signal begins to appear (at $t=240$ s), and the O and Co signals coexist until Co peak disappears, suggesting partial oxidation at the Co/TaOx interface. With increasing t_{Ta}, a clear separation

[a)]Author to whom correspondence should be addressed. Electronic mail: gbeach@mit.edu

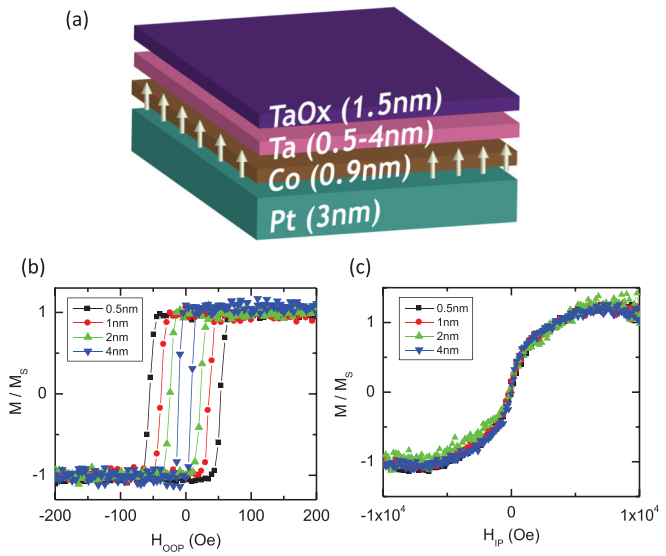

FIG. 1. (a) Schematic Pt/Co/Ta stack structure capped by 1.5 nm of TaOx. The nominal thickness of the Ta top layer varies between 0.5 nm and 4 nm. Normalized out-of-plane (b) and in-plane (c) hysteresis loops were obtained using vibrating sample magnetometry.

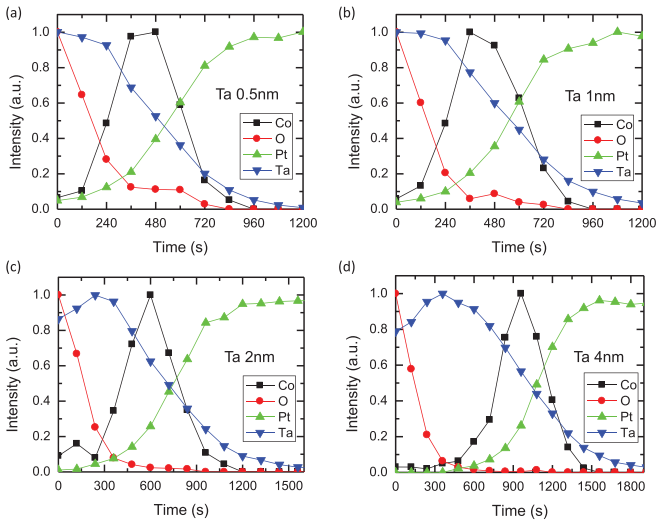

FIG. 2. The normalized intensity of Ta, Co, Pt, and O contributions to XPS spectra versus sputter time for tantalum layer thicknesses t_{Ta} of (a) 0.5 nm, (b) 1 nm, (c) 2 nm, and (d) 4 nm.

exists between the oxide overlayer and the metallic Co layer, indicating direct contact between Co and metallic Ta for thicker t_{Ta}.

We quantified SOTs by detecting current-driven magnetization tilting using harmonic Hall voltage measurements.[28] For these measurements, Hall bar structures were fabricated using electron beam lithography and lift-off, followed by a second lithographic step to deposit Ta(5 nm)/Cu(135 nm) contact pads. In this measurement scheme, the variation of the first and second harmonics of the anomalous Hall voltage with in-plane fields are used to quantify the longitudinal and transverse induced effective fields generated, respectively, by the Slonczewski-like (H_{SL}) and field-like (H_{FL}) SOTs. Figs. 3(a) and 3(b) show schematics of the measurement geometry in each case. An AC injected current generates a periodic torque on the uniformly magnetized Co film, causing the z-component of the magnetization, M_z, to vary at the driving frequency, ω.

The first and second harmonics of the anomalous Hall voltage, V_ω and $V_{2\omega}$, are then measured, while sweeping either a longitudinal field H_L (Fig. 3(a)) or transverse field H_T (Fig. 3(b)), to yield H_{SL} and H_{FL}, respectively, through[28]

$$H_{SL(FL)} = 2\left(\frac{dV_{2\omega}}{dH_{L(T)}}\right) \Big/ \left(\frac{d^2V_\omega}{dH^2_{L(T)}}\right). \quad (1)$$

Here, we define the effective fields in terms of the direction of electron flow, not the direction of conventional current flow, so that the sign differs from Ref. 28.

Measurements were performed at an excitation frequency $\omega/2\pi = 20$ Hz, with the in-plane field swept quasistatically between ± 600 Oe. A small out-of-plane bias field ($\sim$50 Oe) was applied during measurement to prevent magnetization switching and domain nucleation. Figs. 3(c) and 3(d) show exemplary V_ω and $V_{2\omega}$ curves versus H_L at a current density $j_{AC} = 1.8 \times 10^{11}$ A/m^2 for $t_{Ta} = 0.5$ nm, measured both for $M_z > 0$ and $M_z < 0$. Figs. 3(e) and 3(f) show

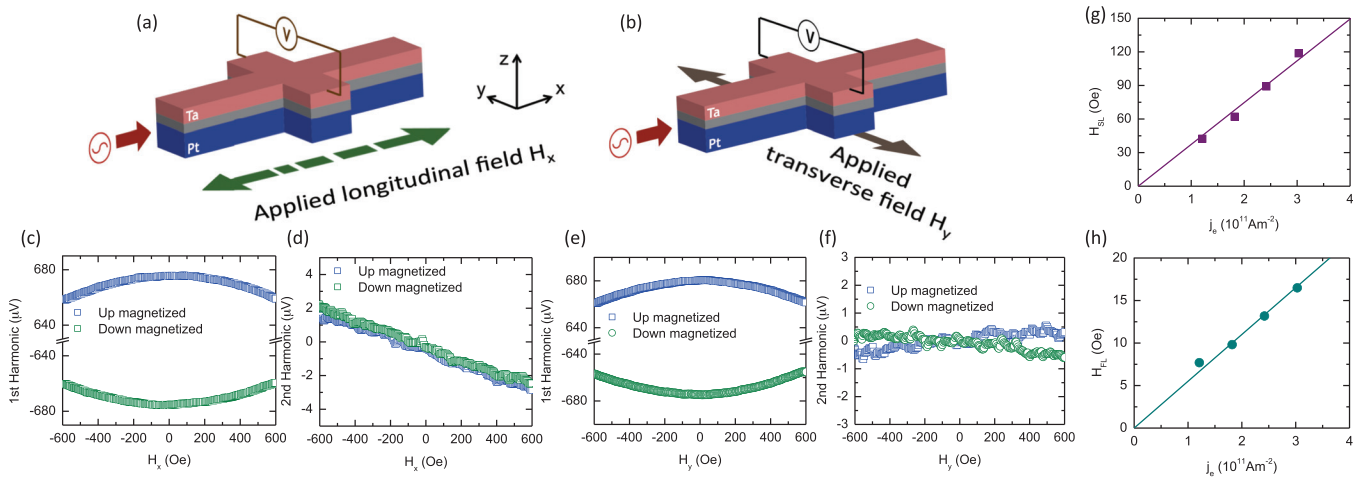

FIG. 3. Schematics of experimental geometry for Slonczewski-like (a) and field-like (b) torque measurement using the ac harmonic technique. Exemplary data for $t_{Ta} = 0.5$ nm showing (c) the first harmonic and (d) second harmonic signals versus longitudinal swept field, and (e) first and (f) second harmonic signals versus transverse swept field. Measurements are shown for both the "up" and "down" magnetized states. The current-induced effective fields versus AC density are shown in (g) for H_{SL}, and (h) for H_{FL}.

corresponding data for H_T. $V_{2\omega}$ varies linearly with $H_{L(T)}$ in this range, and the slope changes sign with M_z for measurements under H_T, but not for H_L, as expected for field-like and Slonczewski-like torques, respectively.[28]

The effective fields H_{SL} and H_{FL}, extracted using Eq. (1), are plotted versus j_{AC} in Figs. 3(g) and 3(h) for $t_{Ta} = 0.5$ nm. The effective fields vary linearly with j_{AC}, indicating that Joule heating or other artefacts that would cause deviations from linearity are negligible within this current range. Similar results were obtained for samples with other t_{Ta}. Fig. 4 shows H_{SL} and H_{FL} per unit current density as a function of t_{Ta}, extracted from the slope of $H_{SL(FL)}$ versus j_{AC}. We find a relatively large H_{SL} that increases from ~30 Oe to ~100 Oe per 10^{11} A/m^2 as t_{Ta} increases from 0.5 nm to 4 nm. H_{FL}, by contrast, is very small at ~5 Oe per 10^{11} A/m^2, and is independent of t_{Ta}.

Since the measured Hall voltage, in general, contains contributions from both the anomalous Hall effect (AHE) and the planar Hall effect (PHE),[29–31] Eq. (1) must be amended if these two contributions are comparable[29–31] since this leads to a mixing of H_{FL} and H_{SL} terms in Eq. (1). We measured both the AHE and PHE resistances (ΔR_A and ΔR_P; see supplementary material for details about PHE measurements[32]), and find a ratio $\xi = \Delta R_P/\Delta R_A \sim 0.3$ for all samples. In this case, the PHE correction is not negligible and should be considered.

The results for H_{FL} and H_{SL} after correcting Eq. (1) for the PHE contribution using the expression given in Ref. 30 (see supplementary material for details regarding PHE correction[32]) are plotted in Fig. 4. We find that the corrected H_{SL} is ~2 times larger than that extracted without taking the PHE into account, and the corrected H_{FL} is comparable to H_{SL}. Intriguingly, we find that the ratio of H_{FL} to H_{SL} is $H_{FL}/H_{SL} \approx 2\xi = 2\Delta R_P/\Delta R_A$, since H_{FL} itself arises almost entirely through the Hall voltage mixing term proportional to ξ in the PHE correction to Eq. (1). This result suggests a relation between SOTs and spin-dependent transport in this system.

Using the PHE-corrected H_{SL}, we computed an effective spin Hall angle to compare the strength of the Slonczewski-like torque in the present system with that in systems based on a single spin Hall-active interface. The effective θ_{SH} was computed from H_{SL} using (Ref. 26) $H_{SL} = \hbar\theta_{SH}|j_e|/(2|e|M_S t_F)$, with t_F is the ferromagnet film thickness, e is the electron charge, and $\hbar$ is the Planck constant. The effective θ_{SH}, plotted in Fig. 4, increases from +0.09 to +0.34 and begins to saturate, as t_{Ta} increases from 0.5 nm to 4 nm, exceeding the record value of 0.30 for W.[4] The value of θ_{SH} for $t_{Ta} = 0.5$ nm is close to that reported for Pt, which is reasonable considering that little if any metallic Ta is likely to remain as a continuous layer at the top interface. As t_{Ta} increases, the effective θ_{SH} also increases. Since the device resistance did not decrease significantly upon addition of t_{Ta}, this suggests that the Ta overlayers include an appreciable fraction of high-resistivity β-phase Ta, which is known to have a large spin Hall angle.[3] However, for the thickest t_{Ta} examined, where Fig. 2(d) shows a significant amount of metallic Ta adjacent to Co, the effective θ_{SH} is considerably larger, exceeding even the sum of $|\theta_{SH}|$ for Pt and β-Ta, which is expected to be ~0.22.[2,3,13,17] We speculate that the presence of Ta within the Co layer and the compositionally graded Co/Ta interface may increase asymmetric spin scattering within the Co layer and/or enhance the spin injection efficiency from the Ta to Co due to the diffuse nature of the interface. However, these points remain to be understood.

Finally, we characterize current-induced switching and extract a measure of the switching efficiency to compare with the effective fields obtained from harmonic SOT measurements. Switching measurements were performed using Hall cross devices, which were 10 μm long and 2 μm wide. Here, a longitudinal bias field H_L was applied to tilt the magnetization along the current axis, so that the Slonczewski effective field[2] $\mathbf{H}_{SL} \propto \mathbf{M} \times (\hat{\mathbf{z}} \times \mathbf{j})$ has a projection along the out-of-plane easy axis that can deterministically switch the magnetization. Switching measurements were performed by first saturating the magnetization along the $-$z direction, and then applying a 100 μs current pulse, after which the magnetization state was measured via the AHE voltage with a small ac sense current. Fig. 5 shows switching phase diagrams in which the mean normalized M_z after current pulse injection was determined for each pair (H_x, j_{pulse}) from ten measurement cycles. The boundary between non-switching and switching is broad due to current-induced nucleation of a metastable nonuniform magnetization texture as described in detail in Ref. 6.

To estimate the switching efficiency, we note that the Slonczewski effective field has an easy-axis (z-axis) component $H_{SL}^z = H_{SL}\sin\varphi$, where φ denotes the angle between $\mathbf{M}$ and the film plane. The equilibrium angle φ for a given H_L is given by $\tan\varphi = H_L/H_k$, where H_k is the perpendicular anisotropy field. We consider that switching should occur at a current density j_{crit} such that $H_{SL}^z = H_c(H_L)$, where $H_c(H_L)$ denotes the coercivity measured in the presence of H_L. Defining $H_{SL} = \chi j$, we arrive at $\chi = H_c(H_L)/j_{crit}\sin\varphi$ as a measure of the switching efficiency. χ was determined for each t_{Ta} by measuring H_c and j_{crit} at $H_L = 1000$ Oe. Due to the broad switching boundary, j_{crit} was taken as the current density for which the mean $M_z = 0$ after current pulse injection. H_k was determined separately for each device by measuring $V_\omega(\propto M_z)$ versus H_x and fitting the data to the Stoner-Wolhfarth model in order to compute φ (see supplementary material for more details[32]).

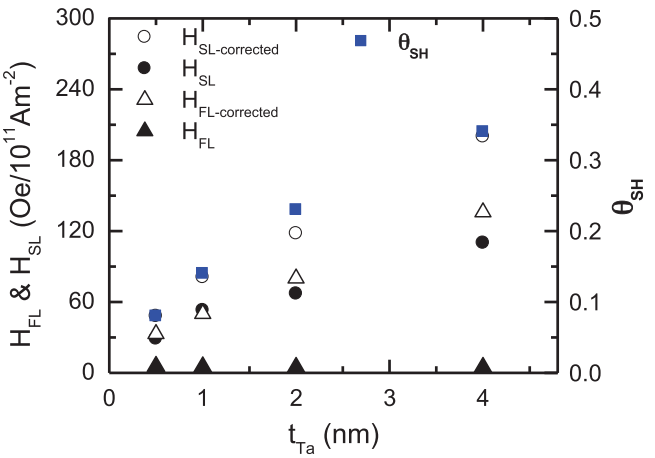

FIG. 4. The effective fields, H_{FL} and H_{SL}, versus the thickness t_{Ta} of the Ta top metal layer (left axis). Results are shown before and after performing the planar Hall effect correction. Effective spin Hall angle computed from the corrected H_{SL} is shown referenced to the right-hand axis.

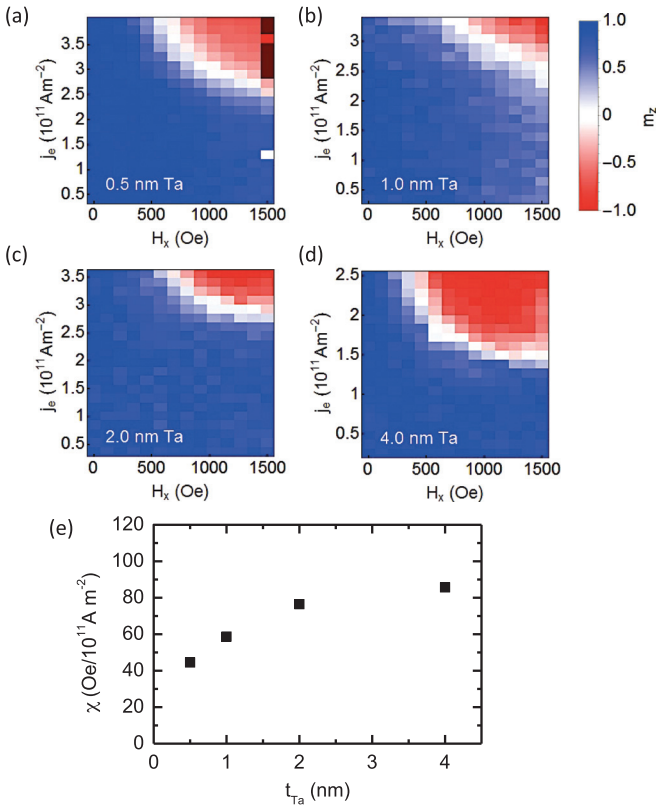

FIG. 5. Switching phase diagrams for Pt/Co/Ta structures with (a) $t_{Ta} = 0.5$ nm, (b) t_{Ta}=1 nm, (c) $t_{Ta} = 2$ nm, and (d) $t_{Ta} = 3$ nm. The color scale denotes the mean normalized out-of-plane magnetization component after current pulse injection, starting from the "down" state. (e) Estimated switching efficiency χ versus t_{Ta}. Note the different current ranges on the vertical axes for panels (a)–(d).

Figure 5(e) shows χ versus t_{Ta}, which exhibits the same qualitative behavior as H_{SL} in Fig. 4. The switching efficiency increases significantly with the addition of a metallic Ta overlayer, by about a factor of 2 over the range of t_{Ta} examined. Notably, χ is consistently less than H_{SL} extracted from harmonic measurements in Fig. 4, which increased by a factor of ~4 for the thickest t_{Ta}. However, it should be emphasized here that this estimate of χ is based on equating field-induced and current-induced switching thresholds. Field-driven reversal can occur by domain nucleation anywhere in the Hall bar, whereas current-induced switching must take place within the Hall cross region, so H_c represents a lower bound on the nucleation threshold corresponding to current-induced switching. Moreover, current-induced nucleation occurs at a current lower than j_{crit}, due to the broad switching boundary. Finally, our analysis of the switching efficiency omits the effects of field-like torque and Dzyaloshinskii-Moriya interaction, which can significantly influence the switching process,[6] so that full micromagnetic simulations would be required for quantitative analysis. Nonetheless, these data show that the H_{SL} enhancement through addition of a Ta overlayer leads to a significant qualitative increase in the current-induced switching efficiency.

We have shown that by sandwiching an ultrathin Co film between heavy metals whose spin Hall angle is of opposite sign, the SOTs from each interface work in concert to enhance the total effective torque. In Pt/Co/Ta, an effective spin Hall angle of 0.34 is achieved, together with a large field-like torque that exceeds 120 Oe per 10^{11} A/m^2. The large enhancement in the Slonczewski-like torque significantly increases the current-induced switching efficiency. Further improvement could likely be obtained by using spin Hall metal pairs with larger spin Hall angles, e.g., by replacing Ta with W. These results point to significant opportunities to engineer the interfaces of ultrathin transition ferromagnets to enhance SOTs for spintronic device applications.

This work was supported in part by the National Science Foundation under NSF-ECCS–1408172, by C-SPIN, one of the six SRC STARnet Centers, sponsored by MARCO and DARPA, and through the SGMI Program. Technical support from David Bono and Elisabeth Shaw was gratefully acknowledged. Work was performed using instruments in the MIT Nanostructures Laboratory, the Scanning Electron-Beam Lithography facility at the Research Laboratory of Electronics, and the Center for Materials Science and Engineering at MIT.

[1]I. M. Miron, K. Garello, G. Gaudin, P.-J. Zermatten, M. V. Costache, S. Auffret, S. Bandiera, B. Rodmacq, A. Schuhl, and P. Gambardella, Nature **476**, 189 (2011).
[2]L. Liu, O. J. Lee, T. J. Gudmundsen, D. C. Ralph, and R. A. Buhrman, Phys. Rev. Lett. **109**, 096602 (2012).
[3]L. Liu, C.-F. Pai, Y. Li, H. W. Tseng, D. C. Ralph, and R. A. Buhrman, Science **336**, 555 (2012).
[4]C.-F. Pai, L. Liu, Y. Li, H. W. Tseng, D. C. Ralph, and R. A. Buhrman, Appl. Phys. Lett. **101**, 122404 (2012).
[5]O. J. Lee, L. Q. Liu, C. F. Pai, Y. Li, H. W. Tseng, P. G. Gowtham, J. P. Park, D. C. Ralph, and R. A. Buhrman, Phys. Rev. B **89**, 024418 (2014).
[6]N. Perez, E. Martinez, L. Torres, S.-H. Woo, S. Emori, and G. S. D. Beach, Appl. Phys. Lett. **104**, 092403 (2014).
[7]G. Yu, P. Upadhyaya, K. L. Wong, W. Jiang, J. G. Alzate, J. Tang, P. K. Amiri, and K. L. Wang, Phys. Rev. B **89**, 104421 (2014).
[8]G. Yu, P. Upadhyaya, Y. Fan, J. G. Alzate, W. Jiang, K. L. Wong, S. Takei, S. A. Bender, L.-T. Chang, Y. Jiang, M. Lang, J. Tang, Y. Wang, Y. Tserkovnyak, P. K. Amiri, and K. L. Wang, Nat. Nanotechnol. **9**, 548 (2014).
[9]T. A. Moore, I. M. Miron, G. Gaudin, G. Serret, S. Auffret, B. Rodmacq, A. Schuhl, S. Pizzini, J. Vogel, and M. Bonfim, Appl. Phys. Lett. **93**, 262504 (2008).
[10]I. M. Miron, P.-J. Zermatten, G. Gaudin, S. Auffret, B. Rodmacq, and A. Schuhl, Phys. Rev. Lett. **102**, 137202 (2009).
[11]I. M. Miron, T. Moore, H. Szambolics, L. D. Buda-Prejbeanu, S. Auffret, B. Rodmacq, S. Pizzini, J. Vogel, M. Bonfim, A. Schuhl, and G. Gaudin, Nat. Mater. **10**, 419 (2011).
[12]S. Emori, D. C. Bono, and G. S. D. Beach, Appl. Phys. Lett. **101**, 042405 (2012).
[13]S. Emori, U. Bauer, S.-M. Ahn, E. Martinez, and G. S. D. Beach, Nat. Mater. **12**, 611 (2013).
[14]K.-S. Ryu, L. Thomas, S.-H. Yang, and S. Parkin, Nat. Nanotechnol. **8**, 527 (2013).
[15]T. Kimura, Y. Otani, T. Sato, S. Takahashi, and S. Maekawa, Phys. Rev. Lett. **98**, 156601 (2007).
[16]K. Ando, S. Takahashi, K. Harii, K. Sasage, J. Ieda, S. Maekawa, and E. Saitoh, Phys. Rev. Lett. **101**, 036601 (2008).
[17]L. Liu, R. A. Buhrman, and D. C. Ralph, e-print arXiv:1111.3702 [cond-mat].
[18]P. P. J. Haazen, E. Murè, J. H. Franken, R. Lavrijsen, H. J. M. Swagten, and B. Koopmans, Nat. Mater. **12**, 299 (2013).
[19]P. Laczkowski, J.-C. Rojas-Sánchez, W. Savero-Torres, H. Jaffrès, N. Reyren, C. Deranlot, L. Notin, C. Beigné, A. Marty, J.-P. Attané, L. Vila, J.-M. George, and A. Fert, Appl. Phys. Lett. **104**, 142403 (2014).
[20]I. M. Miron, G. Gaudin, S. Auffret, B. Rodmacq, A. Schuhl, S. Pizzini, J. Vogel, and P. Gambardella, Nat. Mater. **9**, 230 (2010).
[21]U. H. Pi, K. W. Kim, J. Y. Bae, S. C. Lee, Y. J. Cho, K. S. Kim, and S. Seo, Appl. Phys. Lett. **97**, 162507 (2010).
[22]X. Wang and A. Manchon, Phys. Rev. Lett. **108**, 117201 (2012).

[23]K.-W. Kim, S.-M. Seo, J. Ryu, K.-J. Lee, and H.-W. Lee, Phys. Rev. B **85**, 180404 (2012).
[24]J. C. Slonczewski, J. Magn. Magn. Mater. **247**, 324 (2002).
[25]A. Brataas, A. D. Kent, and H. Ohno, Nat. Mater. **11**, 372 (2012).
[26]A. V. Khvalkovskiy, V. Cros, D. Apalkov, V. Nikitin, M. Krounbi, K. A. Zvezdin, A. Anane, J. Grollier, and A. Fert, Phys. Rev. B **87**, 020402 (2013).
[27]S. Zhang, P. M. Levy, and A. Fert, Phys. Rev. Lett. **88**, 236601 (2002).
[28]J. Kim, J. Sinha, M. Hayashi, M. Yamanouchi, S. Fukami, T. Suzuki, S. Mitani, and H. Ohno, Nat. Mater. **12**, 240 (2013).
[29]K. Garello, I. M. Miron, C. O. Avci, F. Freimuth, Y. Mokrousov, S. Blügel, S. Auffret, O. Boulle, G. Gaudin, and P. Gambardella, Nat. Nanotechnol. **8**, 587 (2013).
[30]M. Hayashi, J. Kim, M. Yamanouchi, and H. Ohno, Phys. Rev. B **89**, 144425 (2014).
[31]X. Qiu, P. Deorani, K. Narayanapillai, K.-S. Lee, K.-J. Lee, H.-W. Lee, and H. Yang, Sci. Rep. **4**, 4491 (2014).
[32]See supplementary material at http://dx.doi.org/10.1063/1.4902529 for details on the XPS measurements and analysis, planar Hall effect correction, and switching efficiency analysis.